

Microstrip Discontinuity Inductances

BRIAN M. NEALE AND A. GOPINATH, MEMBER, IEEE

Abstract—A method of calculation for microstrip discontinuity inductance parameters is described which overcomes various problems encountered in previous methods. A computer program has been written to implement this method, and typical calculated data is presented showing good agreement with experimental measurements.

I. INTRODUCTION

ALTHOUGH several papers have provided a range of results for the capacitive component of microstrip discontinuities [1]–[8], there is still little data available in the literature for the inductive components. Early calculations for these parameters [9], [10] were apparently in error and not confirmed by experimental measurement. The magnetic wall model [11] modified from the method used for triplate lines suffers from a lack of theoretical justification. The inductive components of some discontinuity geometries have been calculated from an approximation-to-quasi-static theory based on the skin effect [12], [13]. The results obtained agree with experimentation only over a restricted range of discontinuities, probably because current continuity through the discontinuity is not always maintained. A second quasi-static formulation [14] sets the normal component of the magnetic field penetrating the strip to zero, which is the normal time-varying boundary condition when the skin effect is fully established. However, these authors used the moment method to obtain the solution, and, as may be seen from their paper, this technique suffers the disadvantage of requiring a large amount of computer store. Additionally, the method cannot be implemented easily for a range of discontinuity geometries.

The present paper follows the formulation set forth in [14] but uses the finite-element technique with polynomial approximations. Thus the computer store requirements are greatly reduced, and, in principle, any microstrip geometry may be studied.

In the following sections we discuss the formulation and method of solution and include some results on T junctions and right-angle bands with experimental measurements for comparison.

Manuscript received October 26, 1977; revised January 16, 1978. This work is supported by the U.K. Ministry of Defence, Procurement Executive under the CVD Directorate. B. M. Neale is supported by an assistantship under this Contract.

The authors are with the School of Electronic Engineering Science, University College of North Wales, Bangor, Gwynedd, U.K.

II. METHOD OF SOLUTION

The method adopted is to calculate the current distribution over the discontinuity structure, subject to appropriate governing and boundary conditions, and from this to obtain the inductance by an analysis of the stored energy in the structure. The quasi-static approximation is assumed neglecting radiation and retardation and implying continuity of current. It is also assumed that the skin effect is completely established. Thus the frequency dependence of the inductance components is not predicted in this work. The governing condition used here is that the normal component of the magnetic flux on the strip is zero which is the normal high-frequency boundary condition.

The discontinuity is described in terms of rectangular elements (as this enables most discontinuities to be described while retaining ease of integration) and semi-infinite lines, which are assumed to exist from $\pm\infty$ to reference planes within the discontinuity. For example, in Fig. 1 both semi-infinite lines terminate at the common plane ss' with no junction region between them. Secondary reference planes are defined at suitable distances from the discontinuity (for example, pp' , qq' in Fig. 1) at which it is assumed that the perturbations due to the discontinuity are negligible and thus beyond which infinite line conditions may be assumed. Continuity of current is maintained through the structure.

The infinite line current distributions are calculated subject to the above governing condition; these currents are assumed to exist up to the planes of termination of the lines. A further current distribution is then calculated over the discontinuity region which redistributes the infinite line currents so that the total current at any point satisfies both governing and boundary conditions. The latter are that perturbations from the infinite line solution are negligible at the secondary reference planes, that current is confined to the conducting strip, and that the continuity of current is maintained across interelement boundaries.

Let us define a current potential \bar{W} such that

$$\bar{J} = \nabla \times \bar{W}$$

where \bar{J} is the current density. We assume the conductor to be a lamina having no variation of current through its thickness. The current density distribution is then characterized by only two components, J_x and J_y . Therefore, it is sufficient for \bar{W} to have a single z -directed component W_z , and hence

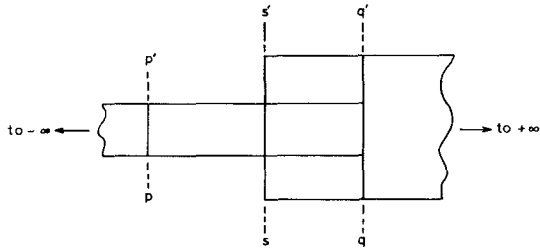


Fig. 1. Typical discontinuity described in terms of rectangular elements.

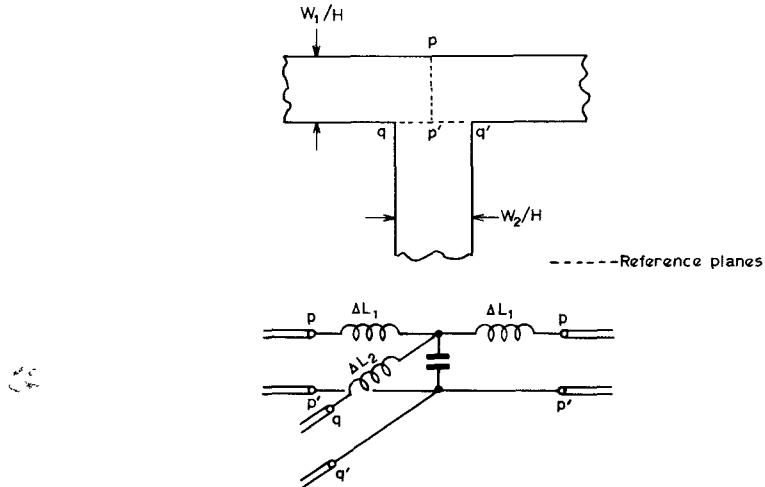


Fig. 2. Reference planes and equivalent circuit for symmetric T junction.

$$J_x = \frac{\partial}{\partial y} W_z$$

and

$$J_y = -\frac{\partial}{\partial x} W_z.$$

In addition,

$$\nabla \cdot \nabla X \bar{W} = 0$$

hence

$$\nabla \cdot \bar{J} = 0.$$

The current so defined is nondivergent and hence continuous.

Now, W_z is described within each element in terms of a trial function set $f_i(x, y)$ defined solely within that element, such that

$$W_z(x, y) = \sum_i a_i f_i(x, y)$$

where a_i is the set of unknown coefficients. The governing equation is set up in matrix form by application of the Galerkin method in terms of these unknown coefficients. Boundary conditions are applied by means of the generalized matrix inverse technique (see the Appendix), which provides a matrix equation relating the original coefficients to a subset of independent coefficients so that any arbitrary choice for these new coefficients will result in a solution satisfying the impressed boundary conditions. The resulting matrix equation is solved to give the independent coefficients, which are then used to evaluate the set a_i as shown in the Appendix.

The discontinuity inductance is calculated from the

relationships

$$I = \int \bar{J} dS$$

and

$$I^2 L = \int \bar{A} \cdot \bar{J} dS$$

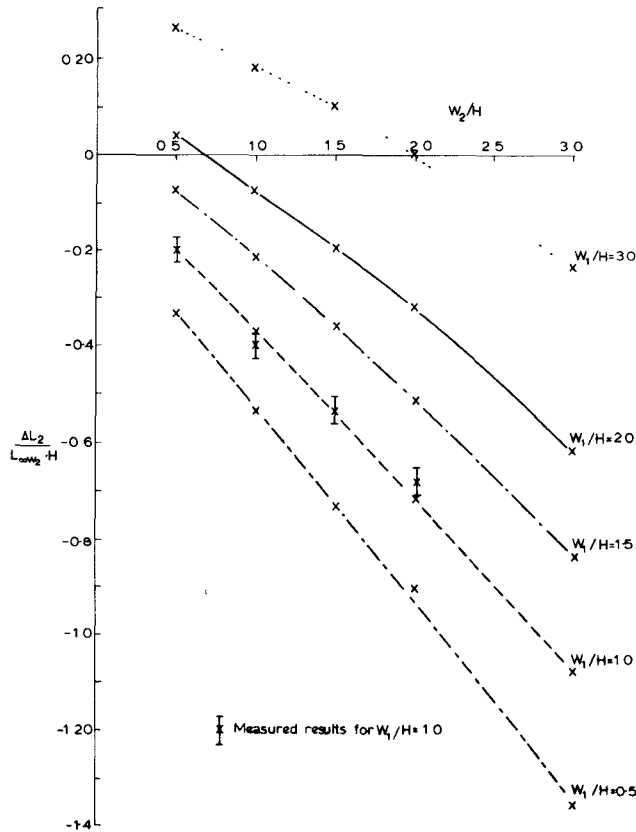
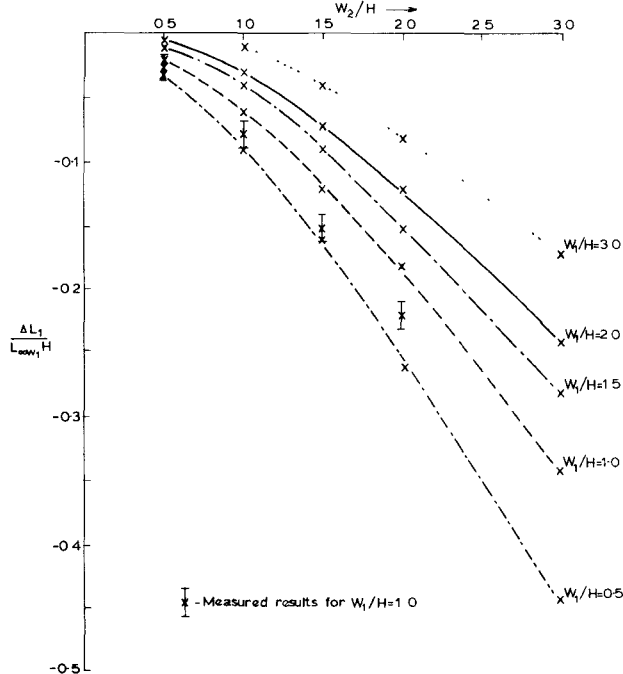
where \bar{A} is the magnetic vector potential. The advantage of describing the current distribution in terms of infinite line and excess (redistributing) components is found in these latter calculations. The discontinuity inductance would otherwise be found by subtracting the infinite line inductance between the secondary reference planes from the total inductance. As the discontinuity inductance is generally much smaller than these two quantities, large numerical errors may arise easily from taking the difference of two nearly equal numbers. Instead, the excess current is itself a measure of the excess inductance, and this enables a more accurate result to be calculated.

In performing the various integrations, both in the governing equation and in the final inductance calculation, mathematical singularities are encountered. These are all handled by coordinate transformation methods analogous to those used by Silvester and Benedek [16].

All numerical integrations are carried out by means of the Gaussian quadrature [17].

III. RESULTS AND DISCUSSION

A computer program has been written to implement the method described above. This program will handle all

Fig. 3. Inductance of straight-through arm of T junction.Fig. 4. Inductance of stub arm of T junction.

discontinuities having rectangular geometries and involving changes in line widths of up to about 1:10. Typical data generated by this program on the T junction and right-angle bend discontinuities are given here. This information, together with the chosen reference planes and equivalent circuits assumed, is set forth in Figs. 2-6. All

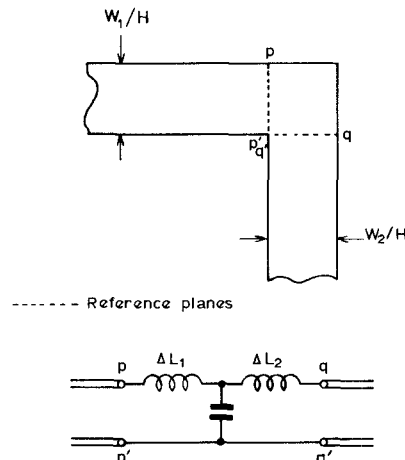
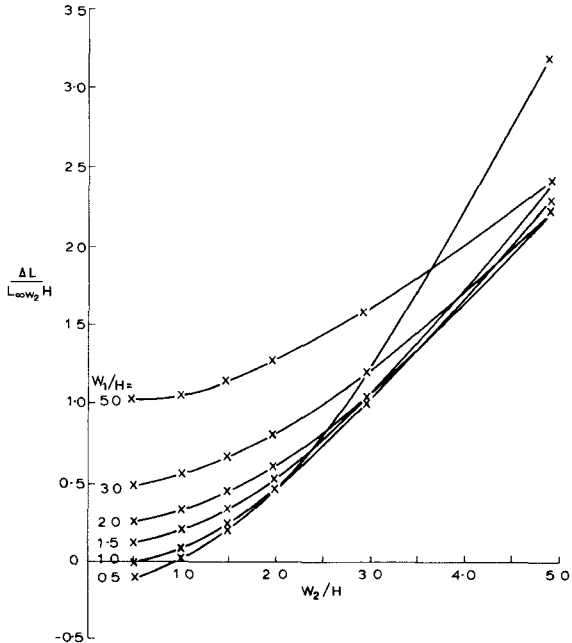


Fig. 5. Reference planes and equivalent circuit for right-angle corner.

Fig. 6. Inductance of right-angle corner ($\Delta L = \Delta L_1 + \Delta L_2$).

results are plotted normalized-to-infinite-line inductance per unit length (L_∞) and substrate height (h). A curve of L_∞ against w/h is given in Fig. 7 for convenience. In the case of the T junction, measured results are given for comparison [6]. Measured and calculated values generally agree to better than an equivalent line length of 15 μm on a 660- μm alumina substrate. This is about the estimated error in the measurements. It should be noted that these results are independent of substrate material provided that it is nonmagnetic.

The program will handle any discontinuity which may be described in terms of rectangular elements. In the case of an n -port junction, the discontinuity may be considered two ports at a time, leaving the others open circuit.

The trial function set used to date has been the bivariate monomial set $1, x, y, x^2, xy, y^2, \dots$ taken to the fourth order. This set has been chosen because it is fast

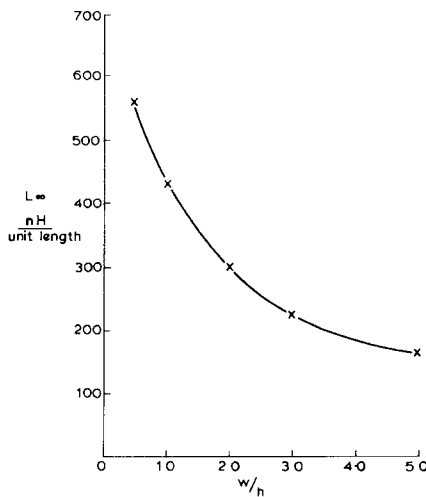


Fig. 7. Inductance per unit length (L_{∞}) of uniform infinite line.

and easy to evaluate at a given point. Its disadvantage is that with high-order approximations it may give poorly conditioned matrices, but this has not been found to be a problem in the present work.

IV. CONCLUSIONS

A finite-element method of calculating quasi-static inductive components of microstrip discontinuities has been outlined. A computer program to perform these calculations has been written, and the results obtained show good agreement with measurements where available. Since the formulation is based on quasi-static assumptions, the data is valid up to some maximum frequency. Experimental observations suggest that this is about 6–8 GHz on 660- μ m alumina substrates (this frequency scales inversely with substrate thickness). Above this frequency, these results form a starting point for designs in the absence of other reliable data. When this data is used in conjunction with the capacitance data available elsewhere, a range of discontinuities is accurately characterized. Inductance results on other discontinuities are currently being collated and will be published in due course.

V. APPENDIX SATISFYING THE BOUNDARY CONDITIONS

The solution of operator equations such as the governing equation described in this paper usually is required to satisfy additionally a set of boundary condition equations. In general, we have

$$[\bar{L}][\bar{a}] = [\bar{g}] \quad (A1)$$

and

$$[B][\bar{a}] = [\bar{b}] \quad (A2)$$

representing the governing equation (commonly set up by some weighted residual technique, for instance) and boundary condition equations, respectively. $[\bar{L}]$ is a square matrix and $[B]$ rectangular. Application of the generalized matrix inversion technique [18] to (A2) allows

us to find further rectangular matrices $[N]$ and $[\bar{k}]$ such that

$$[\bar{a}] = [N][\bar{d}] + [\bar{k}] \quad (A3)$$

where $[N]$ and $[\bar{k}]$ may be determined from (A2). The vector $[\bar{d}]$ represents a new set of basis functions, independent of the boundary conditions. The original set $[\bar{a}]$ is expressed in terms of $[\bar{d}]$ such that any $[\bar{d}]$ together with a constant vector $[\bar{k}]$, which derives from the right-hand side of (A2), will give a vector $[\bar{a}]$ which satisfies the boundary conditions as originally set up in (A2). The rectangular matrix $[N]$ may be considered as a transformation matrix mapping the n -dimensional function space $[\bar{a}]$ into an $(n-m)$ -dimensional function space $[\bar{d}]$ where m is the number of independent boundary conditions specified by $[B]$. Substitution of (A3) into (A1) together with premultiplication of both sides by $[N]$ leads to a system which may be solved for $[\bar{d}]$ and, hence, $[\bar{a}]$ obtained by back substitution in (A3). The resulting solution will, in general, satisfy the boundary conditions exactly and give an approximation to the operator equation. This technique has been found to be both powerful and flexible in the solution of operator equations such as that described in the body of this paper.

The technique has been implemented in the present case using a modified version of the IBM Scientific Subroutine Library package MFGR. Better behaved subroutines for such implementations have also been discussed by Peters and Wilkinson [19].

ACKNOWLEDGMENT

Our thanks are due to B. Easter and Prof. I. M. Stephenson for advice and guidance.

REFERENCES

- [1] A. Farrar and A. T. Adams, "Computation of lumped microstrip capacitances by matrix method—Rectangular sections and end effects," *IEEE Trans. Microwave Theory Tech.*, vol. MTT-19, pp. 495–496, May 1971.
- [2] —, "Matrix method for microstrip three-dimensional problems," *IEEE Trans. Microwave Theory Tech.*, vol. MTT-20, pp. 497–504, Aug. 1972.
- [3] D. S. James and S. H. Tse, "Microstrip end effects," *Electron. Lett.*, vol. 8, pp. 46–47, 1972.
- [4] I. Wolff, "Static capacitances of rectangular and circular microstrip disc capacitors," *Arch. Elek. Übertragung.*, vol. 27, pp. 44–47, 1973.
- [5] Y. Rahmat-Samii, T. Oh, and R. Mittra, "A spectral domain analysis for solving microstrip discontinuity problems," *IEEE Trans. Microwave Theory Tech.*, vol. MTT-22, pp. 372–375, Apr. 1971.
- [6] B. Easter, "The equivalent circuit of some microstrip discontinuities," *IEEE Trans. Microwave Theory Tech.*, vol. MTT-23, pp. 655–660, Aug. 1975.
- [7] C. Gupta and A. Gopinath, "Equivalent circuit capacitance of microstrip step change in width," *IEEE Trans. Microwave Theory Tech.*, vol. MTT-25, pp. 819–822, Oct. 1977.
- [8] C. Gupta, B. Easter, and A. Gopinath, "Some results on the end effects of microstrip lines," to be published.
- [9] R. Horton, "Electrical characterization of a right-angled bend in microstrip line," *IEEE Trans. Microwave Theory Tech.*, vol. MTT-21, pp. 427–429, June 1973.
- [10] —, "Electrical representation of an abrupt impedance step in microstrip line," *IEEE Trans. Microwave Theory Tech.*, vol. MTT-21, pp. 562–564, Aug. 1973.

- [11] I. Wolff, G. Kompa, and R. Mehran, "Calculation method for microstrip discontinuities and *T* junction," *Electron. Lett.*, vol. 8, pp. 177-179, 1972.
- [12] A. Gopinath and P. Silvester, "Calculation of inductance of finite length strips and its variation with frequency," *IEEE Trans. Microwave Theory Tech.*, vol. MTT-21, pp. 380-386, June, 1973.
- [13] A. Gopinath and B. Easter, "Moment method of calculating discontinuity inductance of microstrip right-angled bends," *IEEE Trans. Microwave Theory Tech.*, vol. MTT-22, pp. 880-883, Oct. 1974.
- [14] A. F. Thomson and A. Gopinath, "Calculation of microstrip discontinuity inductances," *IEEE Trans. Microwave Theory Tech.*, vol. MTT-23, pp. 648-655, Aug. 1975.
- [15] P. Silvester, "TEM-wave properties of microstrip transmission lines," *Proc. Inst. Elec. Eng.*, vol. 115, pp. 43-48, Jan. 1968.
- [16] P. Silvester and P. Benedek, "Capacitance of parallel rectangular plates separated by a dielectric sheet," *IEEE Trans. Microwave Theory Tech.*, vol. MTT-20, pp. 504-510, Aug. 1972.
- [17] Stroud and Secrest, *Gaussian Quadrature Formulas*. Englewood Cliffs, NJ: Prentice Hall, 1966.
- [18] Z. Csendes, A. Gopinath and P. Silvester, "Generalised matrix inverse techniques for local approximations of operator equations," in *Mathematics of Finite Elements and Its Applications*, J. Whiteman, Ed. New York: Academic Press.
- [19] G. Peters and J. H. Wilkinson, "The least-squares problem and pseudo-inverses," *Comput. J.*, vol. 13, pp. 308-316, Aug. 1970.

Capacitance Parameters of Discontinuities in Microstriplines

A. GOPINATH, MEMBER, IEEE, AND CHANDRA GUPTA, STUDENT MEMBER, IEEE

Abstract—Capacitance components of microstrip equivalent circuit discontinuities of gaps and the *T* junctions have been calculated using the quasi-static formulation. Comparison of the calculated results with experimental measurements where available show good agreement. The range of data extends that data previously published, and new results on parallel gaps also are included.

I. INTRODUCTION

MICROSTRIP circuits comprise lengths of line and a variety of discontinuities, some examples of which are open circuits, gaps (series and parallel types), *T* junctions, cross junctions, corners, and step changes in width. The implementation of a particular design in microstrip is a cut-and-try process involving several trials before a satisfactory layout is obtained. This is largely due to the inadequate data on discontinuities. The present paper goes some way towards filling this gap by providing a range of data on the capacitance components of the equivalent circuits of some widely used discontinuities.

Manuscript received October 26, 1977; revised January 17, 1978. This work is supported by the U.K. Ministry of Defense, Procurement Executive under CVD Directorate. C. Gupta is supported by a U.C.N.W. scholarship.

The authors are with the School of Electronic Engineering Science, University College of North Wales, Bangor LL57 1UT, North Wales, U.K.

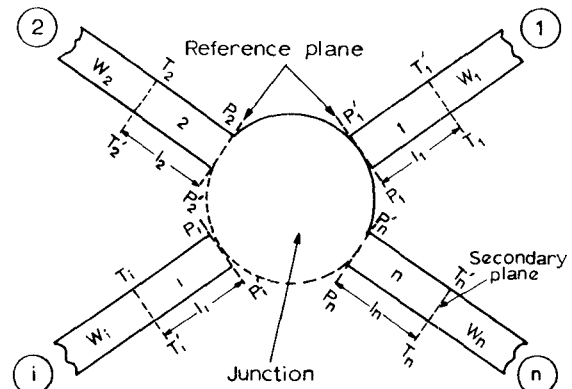


Fig. 1. General microstripline discontinuity.

Several methods of calculating the capacitances associated with discontinuities exist, ranging from quasi-static calculations using the moment method [1], the spectral domain technique [2], and the variational method [3] to the magnetic wall model [4]. The present set of data was generated using the quasi-static approach and the concept of excess charge due to Silvester and Benedek [5]-[7]. The advantage with this method is that the results